## scientific data



### **DATA DESCRIPTOR**

# **OPEN** Comprehensive genome annotation of Trilocha varians, a new model species of Lepidopteran insects

Jung Lee 1 Toshiaki Fujimoto<sup>2,4</sup>, Katsushi Yamaguchi³, Shuji Shigenobu 3, Ken Sahara² & Toru Shimada 101

Trilocha varians is a member of the bombycid moths. Since T. varians has a considerably shorter generation period than the prevailing model species, Bombyx mori, this species would be a novel model insect in Lepidoptera. To facilitate further use of *T. varians*, we developed genome annotation information on the chromosome-scale assembly of T. varians previously published by our group. 9 RNA-seq datasets and 2 Iso-seq datasets were submitted for transcriptome-based gene prediction. As a result, 16,266 protein-coding genes were predicted on the latest genome assembly, and 98.6% of BUSCO sequences were present in our gene models. ATAC-seq was also conducted to determine chromatin accessibility across the genome. Finally, piRNA-targeted small RNA-seg revealed T. varians genome harbours 517 piRNA clusters (piCs). This information will encourage and facilitate potential users who plan to use this species.

#### **Background & Summary**

Trilocha varians (Lepidoptera: Bombycidae; Fig. 1a) is a member of bombycid moths. While in Japan this species was identified for the first time in Okinawa in 2001<sup>1</sup>, T. varians is widely distributed in South and Southeast Asia<sup>2</sup>. Since T. varians lives in low latitude regions, it is a completely non-dormant insect that does not go dormant under any rearing conditions. T. varians mainly feed on banyan leaves, Ficus microcarpa while the domesticated silkworm, Bombyx mori, mainly feed on mulberry leaves. A notable characteristic of this insect is its short generation time. T. varians takes about 30 days at 25 °C and 22 days at 30 °C from hatching to eclosion<sup>3</sup>. In addition, under rearing at 25 °C, eggs hatch in 5 days. Compared to other lepidopteran model species such as Samia ricini<sup>4</sup>, approximately 30 days of generation time is remarkably short, which is a great advantage as a model species.

We have recently published a chromosome-scale female genome assembly of T. varians (NCBI acc: GCA\_030269945.2)<sup>5,6</sup>. Although T. varians genome retains micro and macro synteny to B. mori genome despite several chromosome fusion and fission events, the W chromosome of T. varians does not show any homology to the W chromosome of B. mori. The W chromosome of both species is derived from the Z chromosome<sup>5</sup>, but it is still uncertain whether the W chromosomes of both species are "orthologous" or not. As we have discussed, B. mori and T. varians have different physiological and genetic characteristics, even though they are members of the same family Bombycidae. Providing genome annotation information on *T. varians* will be useful in researching the evolution of the family Bombycidae.

T. varians is 2n = 52 species<sup>3</sup>, and females have 25 pairs of autosomes, Z chromosome, and W chromosome. T. varians used in this study is an inbred strain derived from descendants of females captured at Ishigaki island, Japan, in 2010. Therefore, the heterozygosity in the genome was 0.12% (Fig. 1b). In preparing the annotation

 $^{1}$ Gakushuin University, Faculty of Science, Department of Life Science, Mejiro 1-5-1, Toshima-ku, Tokyo, 171-8588, Japan. <sup>2</sup>Laboratory of Applied Entomology, Faculty of Agriculture, Iwate University, Ueda 3-18-8, Morioka, 020-8550, Japan. <sup>3</sup>National Institute for Basic Biology, Trans-Omics Facility, Nishigonaka 38, Myodaiji, Okazaki, 444-8585, Japan. <sup>4</sup>Present address: Laboratory of Silkworm Genetic Resources, Institute of Genetic Resources, Kyushu University Graduate School of BioResources and Bioenvironmental Science, Motooka 744, Nishi-ku, Fukuoka, 819-0395, Japan. <sup>™</sup>e-mail: yungu.ri@gakushuin.ac.jp

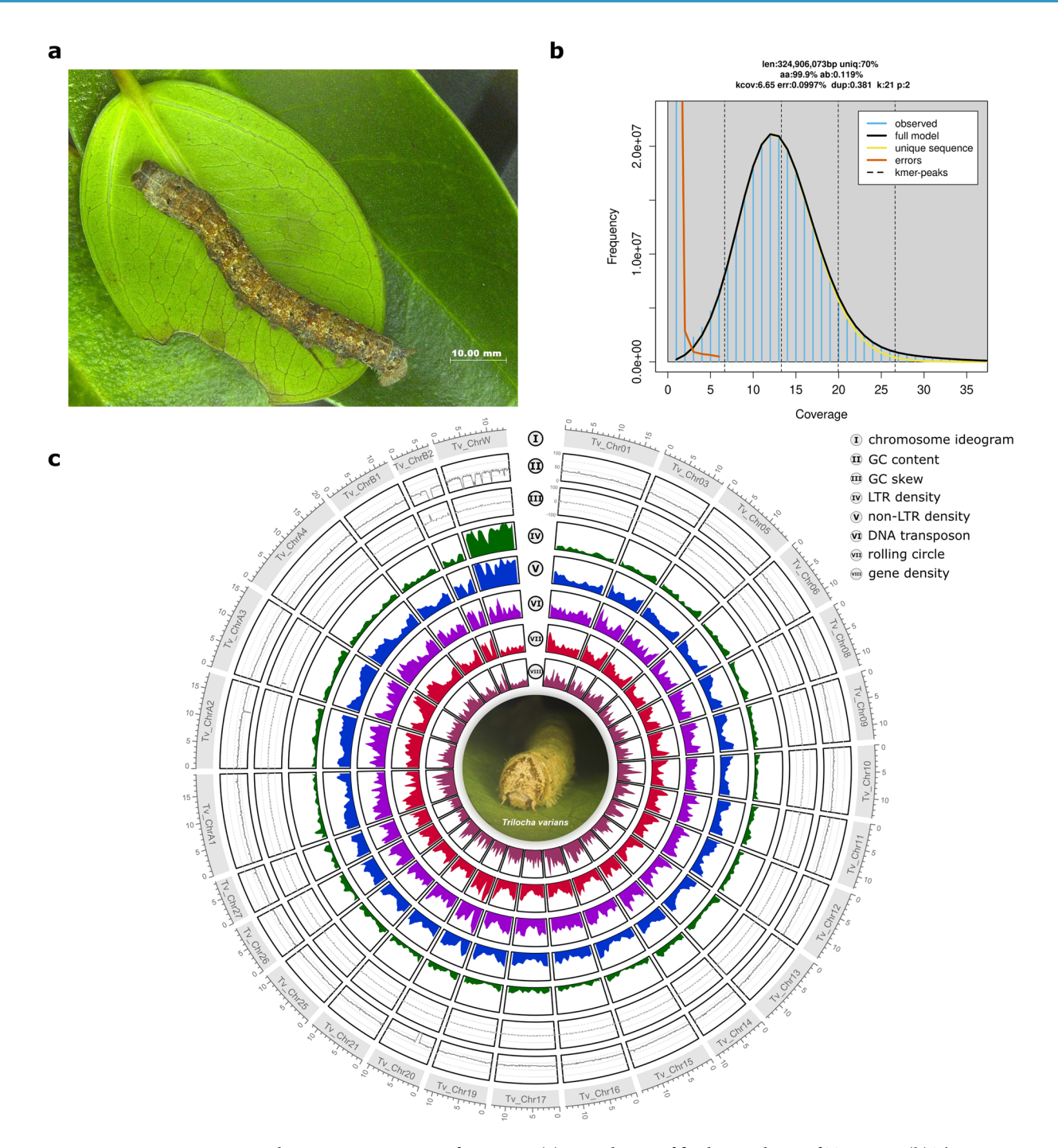


**Fig. 1** General genome annotation information. (a) Dorsal view of final instar larva of *T. varians*. (b) The 21-mer distribution for estimation of genome heterozygosity of *T. varians*. (c) Summary of *T. varians* genome characteristics. The outermost to the innermost circle show the following: I. chromosome ideograms; II. GC content; III. GC skew; IV. LTR element density; V. non-LTR retrotransposon density; VI. DNA transposon density; VII. rolling circle density; and VIII. gene model density.

information, we first attempted to locate the nucleolar organizer region (NOR) because NOR is a region of long repetitive sequences<sup>6</sup>, which often prevent chromosome-scale genome assembly. Transcriptome-based *transcriptome-based* gene prediction identified 16,226 protein-coding genes in *T. varians* genome. The following functional annotation was also performed using EnTAP<sup>7</sup>. Although application examples of CRISPR/ Cas9-mediated genome editing in *T. varians* have not been reported, applying genome editing techniques should be a prerequisite for promoting further use of *T. varians* as a model species. Since Cas9 is known to be less efficient in heterochromatin regions<sup>8</sup>, we performed embryonic ATAC-seq to identify open chromatin regions.

It is known that piRNA is involved in the early development of lepidopteran insects. Although piRNA was originally discovered specifically in germline cells<sup>9–12</sup>, lepidopteran piRNAs are also present in the early embryos. A prominent example of the involvement of piRNAs in early development is *Fem* piRNA of *B. mort*<sup>13</sup>.

Fem piRNA functions as master determinant of female. Although *T. varians* does not have *Fem*, it is known that in diamondback moths, *Plutella xylostella*, W-derived piRNAs are still responsible for female determination <sup>14</sup>. So far, there is no report that embryonic piRNAs are involved in developmental processes other than sex determination. However, the abundance of embryonic piRNAs does not rule out such possibility. To contribute to future piRNA research in *T. varians*, we performed small RNA-seq in early embryos, pupal testes, and pupal ovaries to identify piRNA clusters.

#### Methods

**Insects.** *T. varians* (NBRP strain, derived from individuals caught in Ishigaki Island, Japan)<sup>3</sup> was provided from National BioResource Project-Wild moths (NBRP-Wild moths; http://shigen.nig.ac.jp/wildmoth/). *T. varians* larvae were fed on fresh leaves of *F. microcarpa*. *T. varians* was reared under a long-day condition (16 h light/8 h dark) at 25 °C.

**Estimation of genome heterozygosity.** Heterozygosity of female T. varians genome was estimated using a k-mer (k=21) analysis. Down sampled (to one-tenth) genomic PE short read data derived from female T. varians (accession number: DRR452104)<sup>15</sup> was subjected to Jellyfish (v2.3.0)<sup>16</sup> to count k-mer. k-mer count was plotted by GenomeScope<sup>17</sup> software. The k-mer distribution displays a single peak and the estimated heterozygosity in the genome was 0.119% (Fig. 1a).

Repetitive elements annotation in the genomes. Repetitive annotation of *T. varians* genome was previously defined by our group<sup>5</sup>. To improve readability, the process of repetitive annotation is briefly summarized here: repetitive elements in the genome assembly were identified using RepeatModeler (v 2.0.4)<sup>18</sup> with "-LTRstruct" option for performing an LTR structural search. The annotated elements were masked using RepeatMasker v 4.1.2. (http://www.repeatmasker.org) with default settings. Among the repetitive elements, LTR, non-LTR (LINE or SINE), DNA transposons, and rolling circles were extracted and the density information of those repetitive groups were visualized by circlize (v 0.4.16)<sup>19</sup> (Fig. 1c). GC content and GC skew did not differ significantly among chromosomes, with GC content averaging about 35.6% (Fig. 1c). However, the GC content was higher in the W chromosome, at about 39.0%. This may reflect the characteristics of W chromosomes to accumulate transposons<sup>5</sup> (Fig. 1c).

Construction of a *T. varians* BAC library. Bacterial artificial chromosome (BAC) construction was carried out as previously described<sup>5</sup>. Basically, the procedures were followed according to a method described in Okumura *et al.*<sup>20</sup> with slight modifications<sup>20</sup>. We used male genomic DNAs extracted from *T. varians* pupae (600 mg), and the genomic DNAs were digested with Hind*III* (8–12 U/ml) at 37 °C for 25 min. The digested fragments were fractionated and collected using CHEF Mapper XA pulsed-field gel electrophoresis system (Bio-Rad). The extracted DNA fragments were ligated to the pBeloBAC11 vector, and the ligates were transformed by electroporation (GenePulser II, Bio-Rad) into DH5 $\alpha$  Electro-Cells (TaKaRa). The electroporated cells were spread on L.B. plates containing 12.5 mg/l chloramphenicol (Cm), X-gal, and isopropyl  $\beta$ -D-thiogalactopyranoside. Grown white colonies were stocked in 384-well plates. Stocked plates were stored at -80 °C until further use.

**Chromosome preparations.** Chromosome specimens were prepared using a method described in Yoshido *et al.*<sup>21</sup>. Briefly, ovaries and testes of the last instar larvae of *T. varians* were dissected in a physiological solution, and testes and ovaries were treated with 75 mM and 100 mM KCl solution for 15 min, respectively. After the hypotonic treatment, the testes and ovaries were fixed in Carnoy's fixative (ethanol: chloroform: acetic acid, 6:3:1) for 10 min. Spermatocytes and oocytes were transferred into a 60% acetic acid drop on a glass slide and spread at 55 °C using a heating plate. The preparations were passed through 70%, 80%, and 99% ethanol series, air dried, and stored at -20 °C until time to use.

**BAC-FISH mapping.** Using the STS primer pairs, we selected the BACs according to the methods written in Yoshido *et al.*<sup>21</sup>. The PCR-selected BACs were cultured in 1.5 ml of LB medium containing 20 mg/l chloramphenicol (Cm) for 16 h at 37 °C with a shaking incubator (Bio Shaker BR-23FH, Taitec). Then, plasmid DNA was extracted using a standard alkaline SDS method. BAC-DNA probe (18N21 on Chr11 and 15F13, 17O20 on Chr20, and *Pieris brassicae* 01A06 for NOR detection<sup>19</sup>) labeling and BAC-FISH were performed according to a method described in Yoshido *et al.*<sup>21</sup>. The FISH preparations were counterstained and mounted with Vectashield Antifade Mounting Medium with DAPI (Vector Laboratories). A Leica DM6000B fluorescence microscope (Leica Microsystems) and a DFC350FX black and white charge-coupled device camera (Leica Microsystems) were used for observation and image capturing. The images were processed with Adobe Photoshop 2022. As a result, we successfully located NOR of *T. varians* on chromosome 20 (Fig. 2), while in *B. mori*, the NOR is located on chromosome 11.

RNA sample preparation for sRNA-seq, RNA-seq, and Iso-seq. All RNA samples were prepared exactly as previously described<sup>5</sup>. Total RNA was extracted from multiple embryos, larval, pupal, and adult tissue using TRIzol reagent (Invitrogen) according to the manufacturer's protocol. Embryos were sampled 72 hours after oviposition. Testis and ovary-derived RNA samples were subjected to RNA-seq and sRNA-seq, respectively. Embryonic RNA samples were subjected to sRNA-seq, and Iso-seq, respectively.

**Library preparation for sRNA-seq, RNA-seq, and Iso-seq.** The sRNA-seq library was prepared using TruSeq small RNA kit (Illumina) according to the manufacturer's protocol with a slight modification. To target piRNA, a region of 147–158 nucleotides was extracted in the purification step of the cDNA construct using BluePippin (Sage Science, USA). The constructed library was sequenced on the Illumina HiSeq. 2500 platform

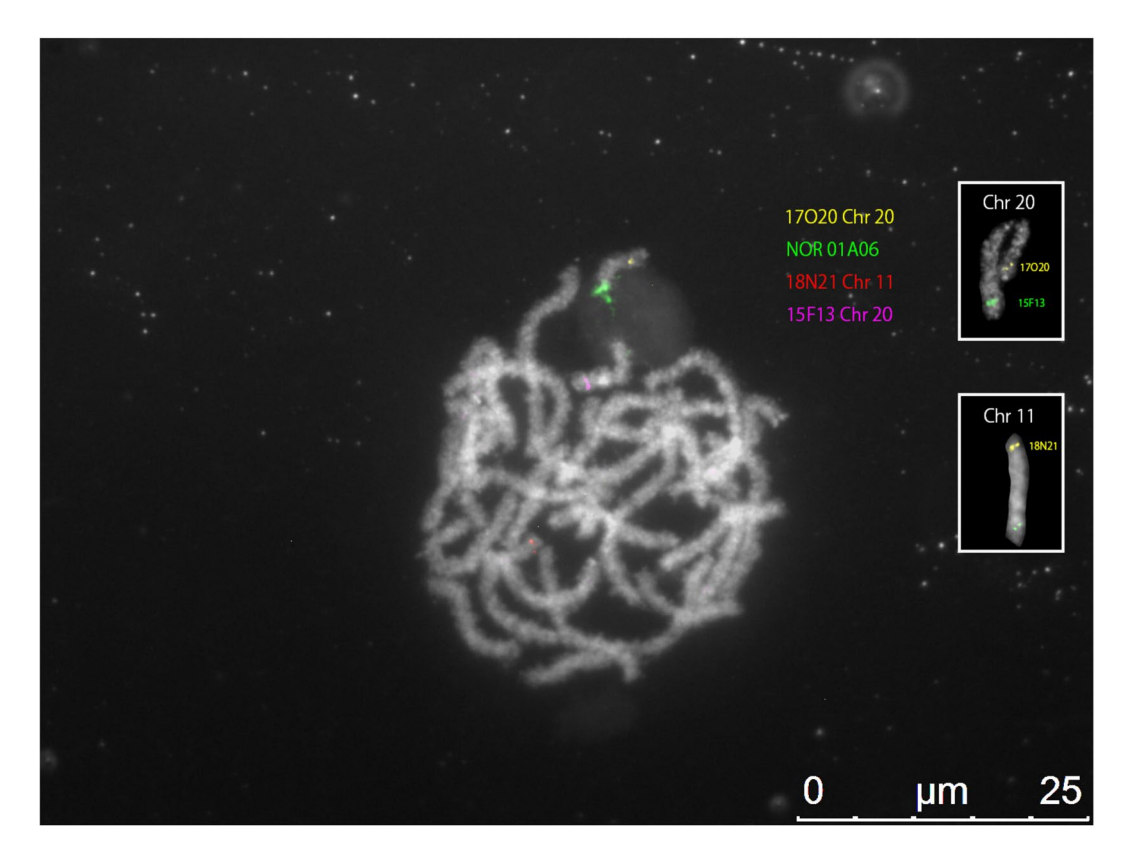


Fig. 2 BAC-FISH mapping of NOR. BAC-FISH mapping was performed using BAC probes 17O20 (yellow), 01A06 (green), 18N21 (red), and 15F13 (magenta) on *T. varians* chromosomes to identify the chromosome location of the NOR. The images of chromosomes 11 and 20 on the right are the results of a previous BAC-FISH analysis using the same BAC (17O20, 18N21, 15F13) (see Lee *et al.*<sup>5</sup>, Fig. 3). The *T. varians* NOR is located in the middle of chromosome 20 while NOR of *Bombyx mori* is located on chromosome 11. Significant chromosome elongation can be observed in the region near the NOR. The picture of chromosome 20 in the top right is from the different sample. This picture shows that the two probes, 17O20 and 15F13, paint the same chromosome. For comparison, a picture of chromosome 11 from the same sample is also shown in the bottom right.

(Illumina, USA). RNA-seq library was prepared using NEBNext Poly(A) mRNA Magnetic Isolation Module (New England BioLabs) and NEBNext® Ultra $^{\text{TM}}$  Il Directional RNA Library Prep Kit (New England BioLabs) according to the manufacturer's protocol. The constructed library was sequenced on the Illumina Novaseq. 6000 platform (Illumina, USA). For Iso-seq, the library was constructed using Sequel Iso-seq Express Template Prep (Pacific Bioscience, USA) according to the manufacturer's protocol. The constructed library was sequenced on the PacBio Sequel platform (PacBio, USA).

**Transcriptome-based gene prediction.** BRAKER3 (v 3.0.8) was used for gene prediction<sup>22,23</sup>. The RNA-seq and Iso-seq data were submitted to BRAKER3 separately<sup>24</sup>, and their respective prediction was finally merged by Tsebra<sup>25</sup>. The detailed information of transcriptome data was summarised in Table 1. Quality trimming for short read data was conducted using fastp (v 0.20.1)<sup>26</sup> with following options: '-q 28 -l 80.' Trimmed short read data were submitted to BRAKER3 using the '-rnaseq\_sets\_ids' option. Then short reads were aligned to the genome assembly by hisat2 (v 2.2.1)<sup>27</sup>. The alignment rates of short read data to the genome assembly were summarised in Table 2. Iso-seq data were generated consensus for each read cluster according to the following procedure<sup>28</sup>: Iso-seq subreads were converted to circular consensus sequences (ccs) using ccs v 6.4.0 with options '-minLength 10-maxLength 100000-minPasses 0-minSnr 2.5-minPredictedAccuracy 0.0.' lima (v 2.7.1) was used to remove primer sequences from the CCSs with options '-isoseq-peek-guess-ignore-biosamples.' After the trimming of adaptors, PolyA tail trimming and concatemer removal were performed by isoseq. 3 v 3.8.2 in 'refine' mode with option '-require-polya.' Finally, isoform-level clustering was conducted by isoseq. 3 in 'cluster' mode with option '-use-qvs.' The resulting clustered.bam file was submitted to BRAKER3. Prior to gene prediction with Iso-seq data, BUSCO analysis on the genome assembly was conducted to obtain complete and single-copy BUSCO sequences<sup>5,29</sup>. Complete and single-copy BUSCO sequences were submitted to BRAKER3 together with Iso-seq derived bam file. Since we had two Iso-seq datasets (Table 1), we ran BRAKER3 for them separately. BUSCO analysis<sup>29</sup> on the constructed gene models scored 98.6% of completeness (Fig. 2a). Basic statistics of the predicted gene models were summarised in Table 3.

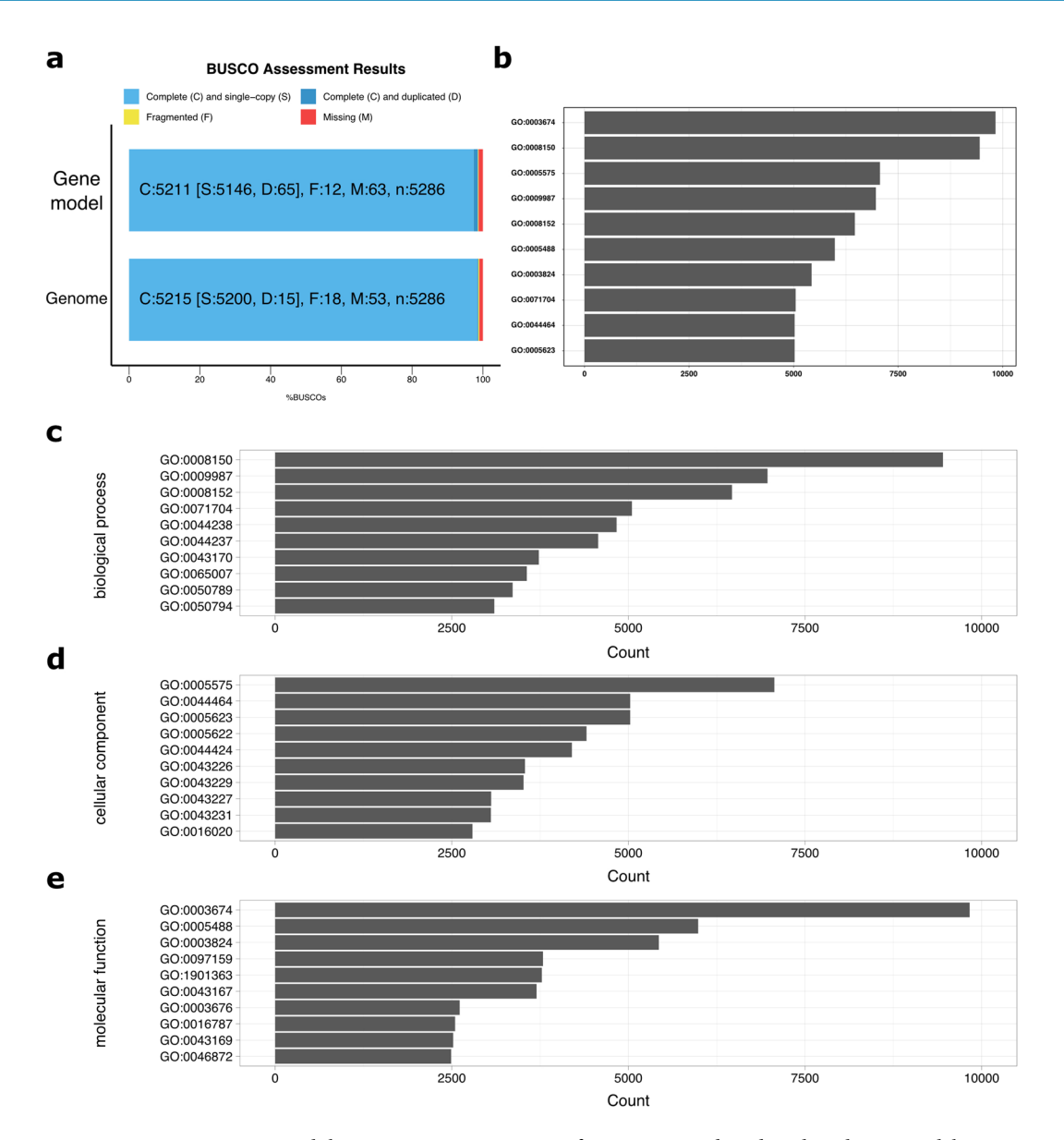


Fig. 3 BUSCO assessment and the top 10 GO assignments of *transcriptome-based* predicted gene models. (a) BUSCO scores of the gene models (top) and the genome assembly (bottom). (b) Overall top 10 GO assignments to gene models. (c) top 10 GO assignments of "biological process" in gene models. (d) top 10 GO assignments of "cellular component" in gene models. (e) top 10 GO assignments of "molecular function" in gene models.

**Functional annotation of gene models.** The deduced amino acid sequences of gene models were submitted to EnTAP<sup>6</sup> for functional annotation. Protein similarity search was conducted against the latest complete UniProtKB/TrEMBL protein data set and complete UniProtKB/Swiss-Prot data set using diamond (v 0.9.14)<sup>30</sup>. Protein orthology search was also conducted against the EggNOG databases<sup>31</sup> to assign Gene Ontology (GO), KEGG terms and protein domains from pfam<sup>32</sup> and smart<sup>33</sup>. Additional family and domain search was performed against tigrfam<sup>34</sup>, sfld<sup>35</sup>, hamap<sup>36</sup>, cdd<sup>37</sup>, superfamily<sup>38</sup>, prints<sup>39</sup>, panther<sup>40</sup>, and gene3d<sup>41</sup> using InterProScan (v 5.68–100)<sup>42</sup>. The results of functional annotation were summarised in Table 4. The top 10 GOs assigned to the gene models are shown in Fig. 3b without distinguishing between molecular function, biological process, and cellular component. The top 10 GOs for each category were shown in Fig. 3c–e.

**ATAC library preparation and data processing.** Another batch of early embryo samples subjected to RNA-seq, Iso-seq, and sRNA-seq were subjected to ATAC-seq. Fragmentation and amplification of the ATAC-seq libraries were conducted according to Buenrostro *et al.*<sup>43</sup>. The constructed libraries were sequenced on the Illumina HiSeq. ATAC-seq reads were pretreated with fastp and mapped to the genome with bwa-mem2 (v 2.2.1)<sup>44</sup>. Alignments containing mismatches were then removed using bamutils (v 0.5.9)<sup>45</sup>. Next, we removed duplicated reads using GATK MarkDuplicates (v 4.1.7)<sup>46</sup>. The resulting bam files were converted to bigwig files

Tissue	No. of spot platform		Read length DRA accession No.		Source	
Larval epidermis	47,924,880	illumina HiSeq	101 PE	DRR574488	this study	
Larval fatbody	60,726,594	illumina HiSeq	101 PE	DRR574489	this study	
Larval malphigian tubules	54,636,622	illumina HiSeq	101 PE	DRR574490	this study	
Larval midgut	41,984,932	illumina HiSeq	101 PE	DRR574491	this study	
Larval nervous system	48,944,178	illumina HiSeq	101 PE	DRR574492	this study	
Adult male antenna	48,000,250	illumina HiSeq	101 PE	DRR574486	this study	
Adult female antenna	52,397,996	illumina HiSeq	101 PE	DRR574487	this study	
Adult pheromone gland	47,710,580	illumina HiSeq	101 PE	DRR574493	this study	
early embryos	15,020,718	illumina HiSeq	150 PE	DRR396188	previously released	
Larval silk gland	14,910,088	PacBio Sequel	Iso-seq	DRR574494	this study	
Early embryos	23,722,715	PacBio Sequel	Iso-seq	DRR396187	previously released	
Early embryos	52,840,298	illumina HiSeq	50 SE	DRR396189	previously released	
Pupal ovaries	25,571,799	illumina HiSeq	50 SE	DRR396190	this study	
Pupal testis	28,138,258 illumina HiSe		50 SE	DRR396191	this study	

Table 1. Transcriptome data used in this study.

Tissue	DRA accession No.	aligned 1 time [%]	aligned > 1 time [%]	not aligned [%]	
Larval epidermis	DRR574488	93.65	4.14	2.21	
Larval fatbody	DRR574489	93.44	3.99	2.57	
Larval malphigian tubules	DRR574490	90.27	5.50	4.23	
Larval midgut	DRR574491	87.47	9.10	3.43	
Larval nervous system	DRR574492	87.74	9.78	2.48	
Adult male antenna	DRR574486	87.42	8.52	4.06	
Adult female antenna	DRR574487	89.11	7.05	3.83	
Adult pheromone gland	DRR574493	87.95	9.47	2.57	
early embryos	DRR396188	89.95	4.67	5.28	

Table 2. Mapping rates of RNA-seq data.

No. of protein coding gene	16,266
Average gene length [bp]	1555.6
Average exon length [bp]	232.23
Average intron length [bp]	1348.95

Table 3. Statistical summary of the constructed gene models.

		Similarity search			Ontology search			
		EggNOG	TrEMBL	Swiss- prot	EggNOG**	InterPro	total	
aligned	Informative	12759	11961	7735	10786	13007	- Annotated***	14481
	Uninformative*	0	2160	183	3095	_		
unaligned		3507	2145	8348	2385	3259	Unannotated***	1785

Table 4. Brief summary of functional annotation. \*When the query sequences were aligned to sequences whose description contains any of conserved/predicted/unnamed/hypothetical/putative/unidentified/ uncharacterized/unknown/uncultured/uninformative, such alignment was categorized as "uninformative", and the query sequence was treated as an unannotated sequence. \*\*In this column, queries with at least one GO term were treated as "Informative", while queries without GO terms were treated as "Uninformative". "Unaligned" in this column means queries without protein family assignment. \*\*\*"Annotated" means at least one match yielded from any the of databases. "Unannotated" means no match yielded from all databases.

using deepTools bamCoverage with 10-bp width bin (v 3.5.1)<sup>47</sup>. The number of reads per bin was normalised by "reads per genomic content" (RPGC) method. Heatmap was created using deepTools computeMatrix with the starting point of the gene model being set to the reference point (Fig. 4).

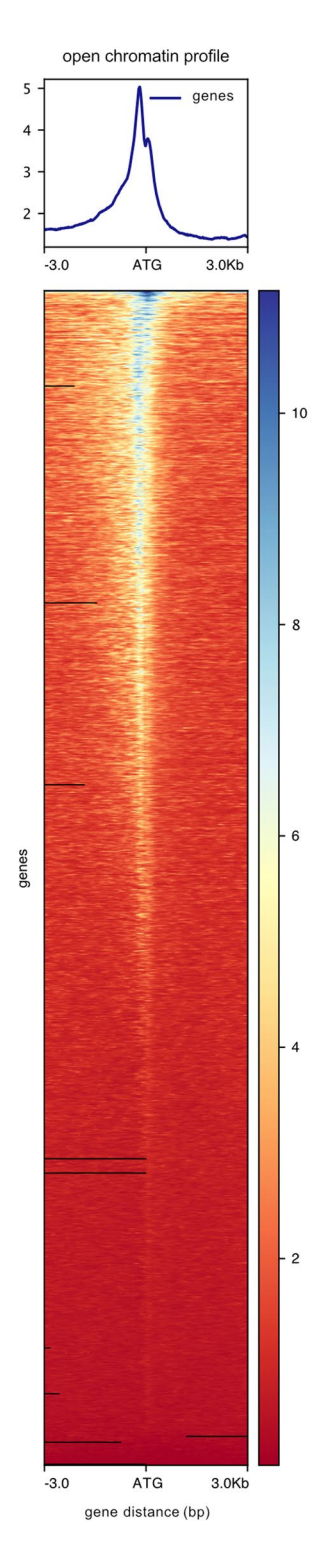


Fig. 4 Heatmap around gene bodies of ATAC-seq on early embryos. The Y axis of the profile plot on the top indicates the normalised read counts per bin (10-bp).

**Small RNA mapping.** The small RNA reads were trimmed using Trim Galore v 0.6.6 (https://github.com/FelixKrueger/TrimGalore) in small RNA mode. The trimmed small RNA reads were mapped to the assembled transcriptome, allowing up to 3 nucleotide mismatches using Hisat2 (v 2.1.0)<sup>27</sup> and ngsutils (v 0.5.9)<sup>45</sup>. The information for each library was summarized in Table 1.

**piRNA cluster detection.** The piC detection was performed as previously described $^5$ . proTRAC (v 2.4.4) $^{48}$  was used with options  $^{\circ}$ -clsize 5000 -pimin 23 -pimax 29 -1Tor10A 0.3 -1Tand10A 0.3 -clstrand 0.0 -clsplit 1.0 -distr

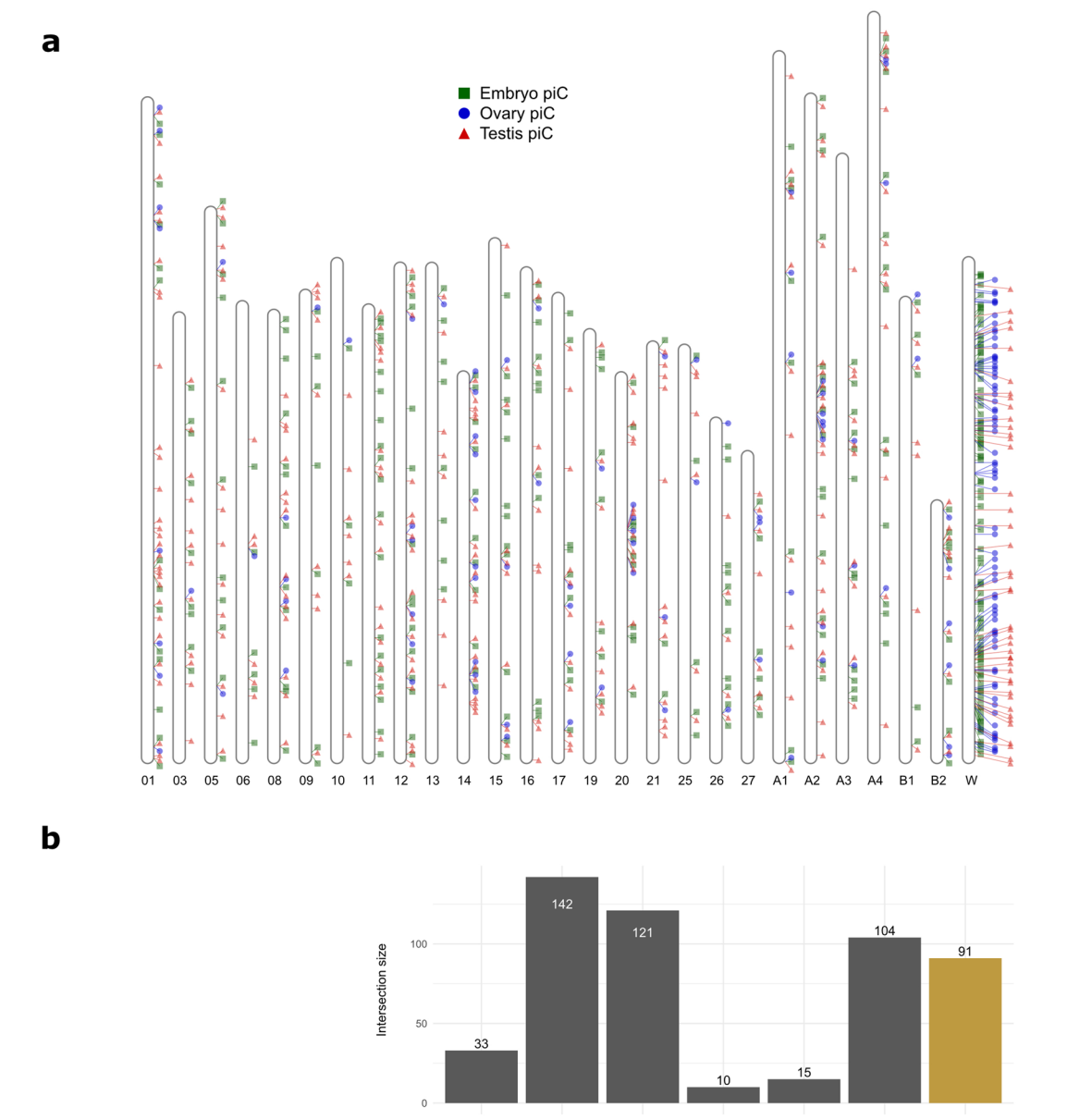


Fig. 5 piRNA clusters on *T. varians* genome. (a) piCs distribution of detected in early embryos (box), pupal ovary (circle), and pupal testis (triangle). (b) UpSet plot visualising piCs that are each assigned to each tissue. The vertical bars correspond to the intersections. When the circles corresponding to tissues are connected by a line, the bar above circles represents the number of piCs commonly identified in concerning tissues. The identity of piCs was defined by the nearest two gene models: When comparing piCs identified in different tissues, if the nearest upstream and downstream gene models are the same, those piCs were treated as the same piC.

piRNA clusters

1.0-99.0 -spike 90-1000 -nomotif -pdens 0.05.' As a result, we successfully identified a total of 517 piRNA clusters in the three tissues (Fig. 5). The identity of a piC is defined by the two nearest (upstream and downstream) gene models. If multiple piCs were predicted between the two gene pair, such piCs were treated as a single piC. The genomic positions of piCs identified in testes, ovaries, and early embryos were visualized by RIdeogram (v 0.2.2)<sup>49</sup> (Fig. 5a). The aggregation relationship of those piCs was visualized by ComplexUpset (v 1.3.3)<sup>50</sup> (Fig. 5b).

#### **Data Records**

The raw sequence data reported in this paper have been deposited in DDBJ. RNA-seq data and Iso-seq data derived from tissues other than early embryos were registered across the accession code PRJDB9419<sup>51</sup>. Embryonic Iso-seq and Embryonic RNA-seq data, small RNA-seq data, and ATAC-seq data are available under the accession code PRJDB13955<sup>52</sup> [DRR396187, DRR396188, DRR396189, DRR396190, DRR396191, DRR515037]. Annotated gene models have been deposited in the figshare repository<sup>53</sup>.

#### **Technical Validation**

To assess the quality of gene models, BUSCO v. 5.4.66 with lepidoptera\_odb10 lineage dataset was used. For comparison, the results are summarized in Fig. 2, together with the results of BUSCO analysis for the genome assembly. 98.58% of the complete and single-copy BUSCO sequences were present in the gene models, while 98.66% of the complete and single-copy BUSCO sequences were present in the genome assembly. BUSCO completeness scores were almost the same between the genome assembly and the gene model, suggesting that the gene prediction process is highly accurate across all genome regions. The mapping rates of RNA-seq data to genome assembly were summarized in Table 1. The mapping rates ranged between 87.5–93.7% for all samples. The mapping rates and the above-mentioned BUSCO completeness scores demonstrate the RNA-seq data quality and the genome assembly quality.

#### Code availability

Programs exploited in this study were executed with the default parameters except where otherwise specified in the Methods section. No custom code was used during this study.

Received: 29 July 2024; Accepted: 5 January 2025;

Published online: 21 January 2025

#### References

- 1. Kishida, Y. Trilocha varians(Walker)(Bombycidae)from Ishigaki Island, the Ryukyu. Japan Heterocerist's J. 219, 370 (2002).
- 2. Soloyevyev, A. V. & Witt, T. J. The Limacodidae of Vietnam (Lepidoptera). Entomofauna 16, 33-229 (2009).
- 3. Daimon, T. *et al.* Molecular Phylogeny, Laboratory Rearing, and Karyotype of the Bombycid Moth, Trilocha varians. *J. Insect Sci.* 12, 1–17 (2012).
- 4. Lee, J. et al. The genome sequence of Samia ricini, a new model species of lepidopteran insect. Mol. Ecol. Resour. 21, 327-339 (2021).
- 5. Lee, J. et al. W chromosome sequences of two bombycid moths provide an insight into the origin of Fem. Mol. Ecol. 33, 1–12 (2024).
- 6. NCBI GenBank https://identifiers.org/ncbi/insdc.gca:GCA\_030269945.2 (2023).
- 7. Hart, A. J. et al. EnTAP: Bringing faster and smarter functional annotation to non-model eukaryotic transcriptomes. *Mol. Ecol. Resour.* 20, 591–604 (2020).
- 8. Jain, S. et al. TALEN outperforms Cas9 in editing heterochromatin target sites. Nat. Commun. 12, 4-13 (2021).
- 9. Aravin, A. et al. A novel class of small RNAs bind to MILI protein in mouse testes. Nature 442, 203–207 (2006).
- 10. Girard, A., Sachidanandam, R., Hannon, G. J. & Carmell, M. A. A germline-specific class of small RNAs binds mammalian Piwi proteins. *Nature* 442, 199–202 (2006).
- 11. Grivna, S. T., Beyret, E., Wang, Z. & Lin, H. A novel class of small RNAs in mouse spermatogenic cells. *Genes Dev.* 20, 1709–1714 (2006).
- 12. Vagin, V. V. et al. A Distinct Small RNA Pathway Silences Selfish Genetic Elements in the Germline. Science (80-.). 313, 320–324 (2006).
- 13. Kiuchi, T. et al. A single female-specific piRNA is the primary determiner of sex in the silkworm. Nature 509, 633-636 (2014).
- 14. Harvey-Samuel, T. et al. Silencing RNAs expressed from W-linked PxyMasc "retrocopies" target that gene during female sex determination in Plutella xylostella. Proc. Natl. Acad. Sci. USA. 119, 1–11 (2022).
- 15. NCBI Sequence Read Archive https://identifiers.org/ncbi/insdc.sra:DRR452104 (2023).
- Marçais, G. & Kingsford, C. A fast, lock-free approach for efficient parallel counting of occurrences of k-mers. Bioinformatics 27, 764-770 (2011).
- 17. Vurture, G. W. et al. GenomeScope: Fast reference-free genome profiling from short reads. Bioinformatics 33, 2202-2204 (2017).
- 18. Flynn, J. M. et al. RepeatModeler2 for automated genomic discovery of transposable element families. *Proc. Natl. Acad. Sci. USA*. 117, 9451–9457 (2020).
- 19. Gu, Z., Gu, L., Eils, R., Schlesner, M. & Brors, B. Circlize implements and enhances circular visualization in *R. Bioinformatics* 30, 2811–2812 (2014).
- 20. Okumura, A. *et al.* Construction of a bacterial artificial chromosome library of Endoclita excrescens as a tool for comparative gene mapping in Lepidoptera. *Entomol. Sci.* 22, 167–172 (2019).
- Yoshido, A., Sahara, K. & Yasukochi, Y. Protocols for cytogenetic mapping of arthropod genomes. in *Protocols for Cytogenetic Mapping of Arthropod Genomes* 381–438, https://doi.org/10.1201/b17450-12 (CRC Press, 2014).
- 22. Stanke, M., Schöffmann, O., Morgenstern, B. & Waack, S. Gene prediction in eukaryotes with a generalized hidden Markov model that uses hints from external sources. *BMC Bioinformatics* 7, 62 (2006).
- 23. Stanke, M., Diekhans, M., Baertsch, R. & Haussler, D. Using native and syntenically mapped cDNA alignments to improve de novo gene finding. *Bioinformatics* 24, 637–644 (2008).
- 24. Lomsadze, A., Burns, P. D. & Borodovsky, M. Integration of mapped RNA-Seq reads into automatic training of eukaryotic gene finding algorithm. *Nucleic Acids Res.* 42, 1–8 (2014).
- 25. Gabriel, L., Hoff, K. J., Brůna, T., Borodovsky, M. & Stanke, M. TSEBRA: transcript selector for BRAKER. *BMC Bioinformatics* 22, 1–12 (2021)
- 26. Chen, S., Zhou, Y., Chen, Y. & Gu, J. Fastp: An ultra-fast all-in-one FASTQ preprocessor. *Bioinformatics* 34, i884–i890 (2018).
- 27. Kim, D., Langmead, B. & Salzberg, S. L. HISAT: a fast spliced aligner with low memory requirements. *Nat. Methods* 12, 357–360 (2015).
- 28. Brůna, T., Gabriel, L. & Hoff, K. J. Navigating Eukaryotic Genome Annotation Pipelines: A Route Map to BRAKER, Galba, and TSEBRA. (2024).
- Manni, M., Berkeley, M. R., Seppey, M., Simão, F. A. & Zdobnov, E. M. BUSCO Update: Novel and Streamlined Workflows along with Broader and Deeper Phylogenetic Coverage for Scoring of Eukaryotic, Prokaryotic, and Viral Genomes. *Mol. Biol. Evol.* 38, 4647–4654 (2021)
- 30. Buchfink, B., Xie, C. & Huson, D. H. Fast and sensitive protein alignment using DIAMOND. Nat. Methods 12, 59-60 (2014).

- 31. Huerta-Cepas, J. et al. EggNOG 5.0: A hierarchical, functionally and phylogenetically annotated orthology resource based on 5090 organisms and 2502 viruses. *Nucleic Acids Res.* 47, D309–D314 (2019).
- 32. Mistry, J. et al. Pfam: The protein families database in 2021. Nucleic Acids Res. 49, D412-D419 (2021).
- 33. Letunic, I. & Bork, P. 20 years of the SMART protein domain annotation resource. Nucleic Acids Res. 46, D493-D496 (2018).
- 34. Haft, D. H. et al. TIGRFAMs: A protein family resource for the functional identification of proteins. Nucleic Acids Res. 29, 41–43 (2001).
- 35. Akiva, E. et al. The Structure-Function Linkage Database. Nucleic Acids Res. 42, 521-530 (2014).
- 36. Pedruzzi, I. et al. HAMAP in 2015: Updates to the protein family classification and annotation system. Nucleic Acids Res. 43, D1064–D1070 (2015).
- 37. Wang, J. et al. The conserved domain database in 2023. Nucleic Acids Res. 51, D384-D388 (2023).
- 38. Pandurangan, A. P., Stahlhacke, J., Oates, M. E., Smithers, B. & Gough, J. The SUPERFAMILY 2.0 database: A significant proteome update and a new webserver. *Nucleic Acids Res.* 47, D490–D494 (2019).
- 39. Attwood, T. K. *et al.* The PRINTS database: A fine-grained protein sequence annotation and analysis resource-its status in 2012. *Database* **2012**, 1–9 (2012).
- 40. Mi, H., Muruganujan, A., Ebert, D., Huang, X. & Thomas, P. D. PANTHER version 14: More genomes, a new PANTHER GO-slim and improvements in enrichment analysis tools. *Nucleic Acids Res.* 47, D419–D426 (2019).
- 41. Lewis, T. E. et al. Gene3D: Extensive prediction of globular domains in proteins. Nucleic Acids Res. 46, D435-D439 (2018).
- 42. Jones, P. et al. InterProScan 5: Genome-scale protein function classification. Bioinformatics 30, 1236-1240 (2014).
- 43. Buenrostro, J., Wu, B., Chang, H. & Greenleaf, W. ATAC-seq method. Curr. Protoc. Mol. Biol. 2015, 1-10 (2016).
- 44. Vasimuddin, M., Misra, S., Li, H. & Aluru, S. Efficient Architecture-Aware Acceleration of BWA-MEM for Multicore Systems. 2019 IEEE Int. Parallel Distrib. Process. Symp. 314–324 (2019).
- 45. Breese, M. R. & Liu, Y. NGSUtils: A software suite for analyzing and manipulating next-generation sequencing datasets. *Bioinformatics* 29, 494–496 (2013).
- 46. van der Auwera, G. & O'Connor, B. D. Genomics in the Cloud: Using Docker, GATK, and WDL in Terra. (O'Reilly Media, Incorporated, 2020).
- 47. Ramírez, F. et al. deepTools2: a next generation web server for deep-sequencing data analysis. Nucleic Acids Res. 44, W160–W165 (2016)
- 48. Rosenkranz, D. & Zischler, H. proTRAC a software for probabilistic piRNA cluster detection, visualization and analysis. *BMC Bioinformatics* 13, 5 (2012).
- 49. Hao, Z. et al. RIdeogram: Drawing SVG graphics to visualize and map genome-wide data on the idiograms. PeerJ Comput. Sci. 6, 1–11 (2020)
- 50. Krassowski, M., Arts, M., Lagger, C. & Max. krassowski/complex-upset: v1.3.5. https://doi.org/10.5281/zenodo.7314197 (2022).
- 51. NCBI Sequence Read Archive http://identifiers.org/ncbi/insdc.sra:DRP008708 (2022).
- 52. NCBI Sequence Read Archive https://identifiers.org/ncbi/insdc.sra:DRP009926 (2023).
- 53. Lee, J. Trilocha varians comprehensive genome annotation information, including gene model, its functional annotation result, and piRNA cluster maps. figshare https://doi.org/10.6084/m9.figshare.23648115 (2024).

#### Acknowledgements

Insects were donated from Kyushu University and Shinshu University according to a Grant-in Aid "National Bio Resource Project (NBRP, RR2002), Silkworm Genetic Resources" for Scientific Research from the Ministry of Education, Science, Sports and Culture of Japan. This study was supported by JSPS KAKENHI Grant Number 24K17900 and 20K15535 to J.L, and JSPS KAKENHI Grant Number J18H03949 to T.S. This study was also supported by the 2022 Gakushuin University Computer Centre Collaborative Research Program to J.L.

### **Author contributions**

J.L. designed the research plan, performed RNA extraction, analyzed the obtained data, and wrote the manuscript. T.S. also designed this research plan and performed the data analysis. T.F. and K.S. performed BAC-clone selection and chromosome imaging. K.Y. and S.S. were in charge of managing the progress of the study and checking and revising the manuscript.

#### **Competing interests**

The authors declare no competing interests.

#### **Additional information**

Correspondence and requests for materials should be addressed to J.L.

Reprints and permissions information is available at www.nature.com/reprints.

**Publisher's note** Springer Nature remains neutral with regard to jurisdictional claims in published maps and institutional affiliations.

Open Access This article is licensed under a Creative Commons Attribution-NonCommercial-NoDerivatives 4.0 International License, which permits any non-commercial use, sharing, distribution and reproduction in any medium or format, as long as you give appropriate credit to the original author(s) and the source, provide a link to the Creative Commons licence, and indicate if you modified the licensed material. You do not have permission under this licence to share adapted material derived from this article or parts of it. The images or other third party material in this article are included in the article's Creative Commons licence, unless indicated otherwise in a credit line to the material. If material is not included in the article's Creative Commons licence and your intended use is not permitted by statutory regulation or exceeds the permitted use, you will need to obtain permission directly from the copyright holder. To view a copy of this licence, visit <a href="https://creativecommons.org/licenses/by-nc-nd/4.0/">https://creativecommons.org/licenses/by-nc-nd/4.0/</a>.

© The Author(s) 2025